Comparison of new bone formation

between biphasic β-TCP bovine vs. β-TCP bovine doped with silicon biomaterials in small and large defects: Experimental study in dogs

Abstract

Objective

The aim of this study was to assess the bone regeneration of critical-size mandibular defects filled with beta-tricalcium phosphate (β-TCP) bovine biomaterial in dogs compared with β-TCP bovine biomaterial doped with silicon at 12 weeks.

Materials and methods

The mandibular second, third and fourth premolars of six Beagle dogs extracted bilaterally were used in this study. Three experimental groups were evaluated: Test A (hydroxyapatite [HA]/β-TCP granules alone), Test B (HA/β-TCP granules plus 3% silicon) and controls (empty defect). The animals were sacrificed at eight and 12 weeks. Evaluation was performed by scanning electron microscopy, X-ray microtomography (μCT) and histological and histomorphometric analysis.

Results

Histological evaluation showed a higher volume reduction in Test A compared with Test B ($p < 0.05$). Test B showed the highest values for cortical defect closure and bone formation around the granules, followed by Test A and the control group ($p < 0.05$).

Conclusion

Within the limitations of this animal study, it can be concluded that HA/β-TCP plus 3% silicon increases bone formation in critical-size defects and the incorporation of 3% silicon reduces the resorption rate of the HA/β-TCP granules.

Keywords

Bone graft, bone substitute, β-TCP, bone defect, dog, silicon.

Introduction

The reconstruction of osseous defects remains an important and unresolved issue in oral surgery. During the first year after tooth extraction, about 50% of the buccolingual ridge dimension will be lost.[1] Healing processes after dental extractions include the formation and maturation of blood clots, the infiltration of immature mesenchymal cells and the formation of a provisional bone matrix.[2] Immature bone becomes established quite early on in this process to be replaced later by mature trabecular bone.[3] Processes of hard-tissue modeling and remodeling after tooth extraction have been studied in the dog model.[4, 5] It was demonstrated that the socket was first occupied by a coagulum that was replaced by granulation tissue, provisional connective tissue and woven bone. More often during this healing period, bone loss occurs in the walls surrounding an extraction site with a reduction in the buccal alveolar crest.[6–8]

There are various alternatives available for the treatment of these osseous defects, the most traditional and long established of these being autogenous bone grafts, used to replace the lost bone. However, this technique has certain disadvantages given that the quantity of available bone is always limited and that it involves a second surgical site and thus increased cost and treatment time and may lead to further problems at the bone graft donor site, such as bleeding, infection and pain. For this reason, different graft materials have been developed that are intended to bring about new bone formation.[9–12]

Among the alternatives available (allografts, xenografts or synthetic bone substitutes), synthetic materials can be ideal for bone regeneration given that many characteristics of such materials—mechanical properties, porosity, degradation rate and composition—can be modified according to the specific clinical requirements.[13,14]

Biomaterial of porcine origin, which has high biocompatibility, stimulates the formation of new bone in contact with biomaterial particles. This material is used for maxillary sinus elevation prior to implant placement.[15–17]

According to Tadic and Epple, synthetic calcium phosphate bone substitutes, such as hydroxyapatite (HA), tricalcium phosphate (TCP) and biphasic calcium phosphate (BCP), offer excellent biocompatibility and are in common use as alternatives to autologous bone.[18] In particular, BCP ceramics, consisting of mixtures of HA and beta-tricalcium phosphate (β-TCP), are widely used as bone substitutes. Although BCP and β-TCP are more resorbable than HA bioceramics, an even higher resorption rate is desirable for bone repair applications whenever complete implant osseointegration and bone replacement are required in the midterm.

Recently, ceramics doped with silicon at different rates have become a subject for research because of the biological benefits of silicon in their chemical composition.[19] Zou et al. have reported that silicon-doped BCP enhances osteoconductivity and has been found to be nontoxic *in vivo* at concentrations as high as 50,000 ppm, producing no adverse effects in rats.[20]

Furthermore, it has recently been postulated that silicon in the form of nanoparticles could even be bioactive and beneficial to the skeleton, although the mechanisms by which silicates regulate skeletal development and function remain unknown.[21] The addition of silicon to TCP can improve stability, provide better structural properties and stimulate new bone formation in small animal models.[22, 19] The literature, however, includes few examples of *in vivo* research into the benefits of incorporating 3% silicon nanoparticles into HA/β-TCP porous granular structures.

The purpose of this *in vivo* study was to evaluate the biological effects of the incorporation of 3% silicon nanoparticles into HA/β-TCP by histological and histomorphometric analysis, scanning electron microscopy and X-ray microtomography (μCT) evaluation in canine bone defects.

Materials & methods

Animals

Six male beagle dogs of 1.5 years of age and weighing 12–13 kg each were used in the study. The experiment protocol was designed in accordance with the Spanish and European guidelines for animal experiments. The experiment was approved by the Ethics Committee for Animal Research of the University of Murcia (Spain), in accordance with the European Union Council Directive of Feb. 1, 2013 (R.D.53/2013).

Surgical procedure

The animals were pre-anesthetized with acepromazine (0.12%–0.25 mg/kg), buprenorphine (0.01 mg/kg) and medetomidine (35 mg/kg). The mixture was injected intramuscularly into the femoral quadriceps. Then an intravenous catheter was inserted (22- or 20-gauge diameter) into the cephalic vein, and propofol was infused at a slow constant infusion rate of 0.4 mg/kg/min. Conventional dental infiltration anesthetic (articaine 40 mg, 1% epinephrine) was administered at the surgical sites. These procedures were carried out under the supervision of a veterinary surgeon.

Teeth extraction and grafting procedures

In both quadrants of the lower jaws, the second, third and fourth premolars (PM) and first molars (M1) were used as experimental sites. The alveoli corresponding to PM2, PM3 and PM4 were classified as small defects and M1 as large defects, respectively.

Teeth were sectioned with a carbide tungsten drill; the roots were removed with forceps, without damaging the remaining bony walls. Sulcular marginal incisions were made along the vestibular and lingual areas adjoining the alveoli, separating tissues to make the crestal hard-tissue walls visible **(Figs. 1a & b)**.

Prior to graft placement, the external dimensions of the post-extraction sockets (diameter) were measured using a caliper and recorded. The mean alveolar ridge measurements of the extraction sockets were as follows: 3.8 ± 0.21 mm (PM2), 4.0 ± 0.5 mm (PM3), 4.1 ± 1 mm (PM4) and 5.6 ± 0.07 mm (M1).

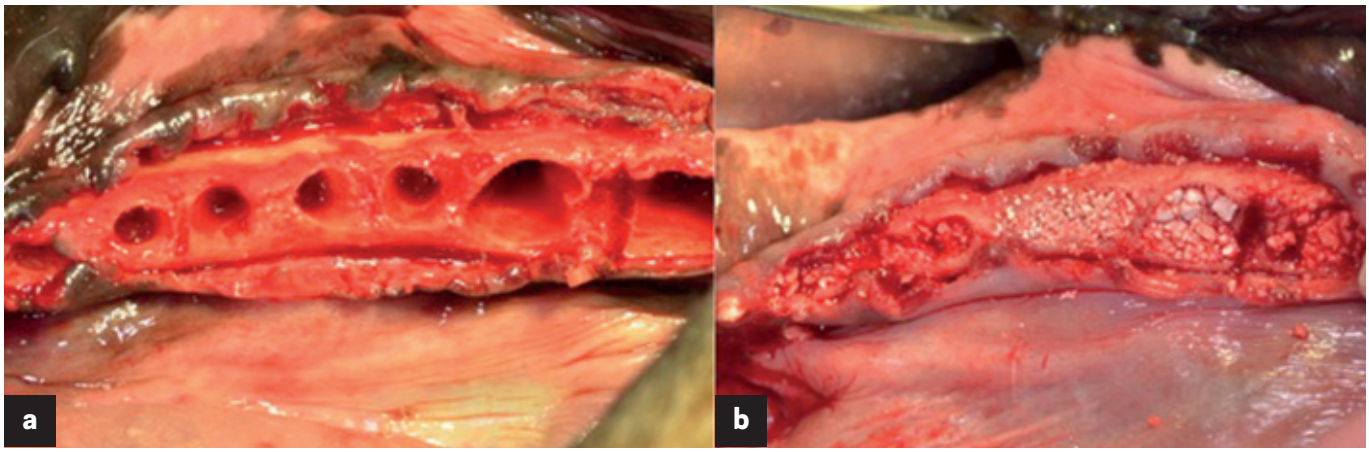

Figs. 1a & b

Figs. 1a & b

Post-extraction sockets of premolars PM2, PM3, PM4 and molar M1 **(a)**; 4BONE XBM granules, 4BONE XBM plus 3% silicon and control sites **(b)**.

Biomaterials

The study used 4BONE XBM granules (MIS Implants Technologies, Bar-Lev, Israel), a widely available bone substitute. This material consists of a completely synthetic bone graft material composed of 60% HA and 40% β-TCP, and features 70% interconnected macroporosity and microporosity. It is available as granules of 0.5–1 mm in size and is packaged in syringes that must be hydrated with physiological saline prior to use (following the manufacturer's instructions; Fig. 1b). Two different forms of this material were used: 4BONE XBM bovine granules in their manufactured form (without modification) and 4BONE XBM bovine granules plus 3% silicon, which was prepared by immersing 50 g of 4BONE XBM sequentially in a liquid solution containing 3% silicon nanoparticles for 2 h. Afterwards, the hydrated granules obtained were heated to 134 °C for 1 h to dry the liquid content and to sterilize the material prior to use.

Synthesis of hydroxyapatite

Hydroxyapatite was synthesized by solid-state reaction from a stoichiometric mixture of anhydrous calcium hydrogen phosphate ($CaHPO_4$, Sigma-Aldrich, St. Louis, Mo., U.S.) and calcium carbonate ($CaCO_3$, Sigma-Aldrich, St. Louis, Mo., U.S.) with an average particle size of < 15 µm and a Ca/P ratio of 1.72. The mixture of $CaHPO_4$ and $CaCO_3$ was heated in a platinum crucible at 1,200 °C for 6 h at a heating rate of 10 °C/min, followed by cooling at a rate of 6.5 °C/min until it had reached room temperature. The obtained material was ground and characterized by X-ray diffraction.

Synthesis of tricalcium phosphate

Tricalcium phosphate was synthesized by solid-state reaction from a stoichiometric mixture of anhydrous $CaHPO_4$ (Panreac, Barcelona, Spain) and $CaCO_3$ (Fluka) with an average particle size of < 15 µm and a Ca/P ratio of 1.60. The mixture of $CaHPO_4$ and $CaCO_3$ was heated in a platinum crucible at 1,000 °C for 12 h, followed by slow cooling. The obtained material was ground and characterized by X-ray diffraction.

Study design

The alveoli (small defects and large defects) corresponding to the right hemi-mandible were used as controls and were filled with 4BONE XBM granules, after rehydration with sterile saline, and the left hemi-mandible defects (small defects and large defects) were filled with 4BONE XBM granules doped with 3% silicon as a second test material. In summary, three treatment groups were created:

(i) bone defects filled with 4BONE XBM granules alone (Test A)
(ii) small defects filled with 4BONE XBM granules doped with 3% silicon (Test B)
(iii) control bone defects.

Samples were allocated to test groups using randomization software (Research Randomizer).[23]

Tissue flaps were repositioned without tension-free adaptation using interrupted and horizontal mattress sutures for wound closure (Monofil 4-0, Ancladén, Barcelona, Spain). During the first week after surgery, the animals were medicated with amoxicillin (500 mg b.i.d.) and

ibuprofen 600 mg t.i.d.) administered systemically. The sutures were removed after two weeks. The dogs received a soft diet and a plaque control regimen that included tooth cleaning with the use of toothbrush and dentifrice, and administration of a 0.2% chlorhexidine solution three times a week until the end of the experiment (eight and 12 weeks).

Table 1

Residual volume	8 weeks (Mean ± S.D.)	12 weeks (Mean ± S.D.)
Test A	63.72 ± 5.1 %	43.91 ± 1.2 %
Test B	76.22 ± 1.6 %*	58.53 ± 1.1 %*

Statistical significance was set at $p < 0.05$.

Table 1
Residual volume of graft material at eight and 12 weeks.

At 12 weeks, both test groups showed a reduction in the volume of material in comparison with eight weeks.

Test B showed slower resorption expressed as higher residual volume in comparison with **Test A** at eight and 12 weeks.

Animal euthanasia

The animals were euthanized at eight (three animals) and 12 weeks (three animals) by means of an overdose of Sodium Pentothal (Abbott Laboratories, Chicago, Ill., U.S.).

Micro-CT evaluation

Immediately after sacrifice at eight or 12 weeks, μCT evaluation was performed to evaluate the residual volume of graft material. Each specimen was placed on the scanning platform of a GE eXplore Locus μCT scanner (GE Healthcare, Piscataway, N.J., U.S.) and 360 X-ray projections were collected (80 kVp, 500 mA, 26 min total scan time). The projection images were preprocessed and reconstructed into 3-D volumes (20 μm resolution). Each volume was scaled to Hounsfield units using a calibration phantom containing air and water (phantom plastic); a plug within the phantom containing HA was used as a bone mimic for bone mineral/density calculations. The 3-D data was processed and rendered (isosurface/maximum intensity projections) using MicroView (GE Healthcare). Volumes were imported into MATLAB (R2009b, MathWorks, Natick, Mass., U.S.) for automated batch analysis. Briefly, a fixed cylindrical volume of interest (14 mm diameter, 5 mm height) was applied to each volume. As each volume was calibrated using a fixed standard, calcium phosphate, cortical bone, trabecular/woven bone and scaffold content were determined using predefined Hounsfield unit thresholds (> 3,000, 2,000–3,000, 750–2,000, and 300–750, respectively).

Residual graft material was calculated as the graft/total bone volume × 100, expressed as a percentage at eight or 12 weeks for both test groups **(Table 1)**.

Sample processing

The soft tissue of each mandible was dissected to leave exposed the bone surfaces. Each mandible was block-sectioned and the tissue fixed with 4% formalin. The samples were dehydrated in a graded ethanol series. The blocks were infiltrated with Technovit 7200 resin (Heraeus Kulzer, Hanau, Germany) and polymerized with ultraviolet light.

The polymerized blocks were then sectioned in a buccolingual direction. Three slices were obtained per site and reduced by micro-grinding and polishing using an EXAKT grinding unit (EXAKT, Norderstedt, Germany) to an even thickness of approximately 15–30 lm. The slides were stained with the Lévai–Laczkó technique; the entire circumference of each section (containing bone, grafted granules and connective tissue) was traced manually to create individual regions of interest.

Histomorphometric analysis

The percentages of residual graft material, connective tissue and new bone were calculated in relation to the total measurement area (socket walls). The central portion of each core was selected to avoid any potential bias. In this way, both the coronal (remaining native host bone) and the apical portions were excluded from analysis (using a safe margin of 1.5–2 mm). Histomorphometric measurement of the samples was conducted using ImageJ software (developed by the U.S. National Institutes of Health, Bethesda, Md.). Descriptive evaluation and morphometric measurements were performed under a Nikon Eclipse 80i microscope (Tekno Optik, Huddinge, Sweden) equipped with the Easy Image 2000 system (Tekno Optik) using 91–94 lenses **(Fig. 2)**.

Histomorphometric evaluation

Prepared samples were photographed with a digital camera using a 20× motorized optical microscope (BX51, Olympus, Japan). These photographs were combined using computer software (cellSens Dimension, Olympus, Japan) to

Fig. 2

Fig. 2
Region of interest (ROI)

Each defect was identified by one orifice marked with amalgam. The ROI was a polygon delimited by the lateral walls of the defect on both sides, coronally by the upper cortical and inferiorly by the basal cortical (5× magnification, Lévai–Laczkó staining).
CDC = cortical defect closure;
CT = connective tissue;
NB = new bone;
MB = mature bone.

obtain high-resolution images of the entire sample. Regions of interest (ROI) were manually delimited to facilitate identification of the different tissues present in each sample. The following variables were recorded at the two study times (eight and 12 weeks):

Cortical defect closure: Percentage of new bone present within the original defect walls in the ROI.
Residual material: Percentage of granules present inside the ROI in relation to the total area **(Fig. 2)**.
Connective tissue: Connective tissue or the connective tissue space present inside the ROI expressed as percentage.
New bone: Percentage of new bone present inside the marrow space and between the granules in the ROI.

Statistical analysis

Statistical analysis was performed using IBM SPSS Statistics software (Version 20.0; IBM Corp., Armonk, N.Y., U.S.). After descriptive analysis, the Mann–Whitney *U* test was used to evaluate the significance of differences between Test A and Test B.

The Friedman test is the nonparametric equivalent of a one-sample repeated measures design or a two-way analysis of variance with one observation per cell. Values were recorded as mean ± standard deviation. The Student's *t*-test was applied to compare mean averages and to quantify relationships between differences.

Friedman tests the null hypothesis that *k* related variables come from the same population. For each case, *k* variables are assigned the rank 1 to *k*. The statistic is based on these ranks. Equal means were regarded as the null hypothesis, while the existence of significant differences between means acted as an alternative hypothesis. As significant differences between the means did exist, the null hypothesis was rejected. Significance was set at $p < 0.05$.

Results

At eight and 12 weeks, no animals had been lost and the surgical zones showed no signs of inflammation. In all experimental sites, healing was uneventful. After eight and 12 weeks of healing, keratinized mucosa was observed covering the edentulous zones without dehiscences or exposure of bone or graft granules. The histomorphometric and histological results of new bone formation, residual graft and connective tissue after eight and 12 weeks of healing are described below.

Micro-CT evaluation

At eight weeks, Test B showed a higher residual volume of graft material (76.22 ± 1.6%) in comparison with Test A (63.72 ± 5.1%; **Figs. 3a–c**). A higher reduction in volume was observed at 12 weeks in Test B, which maintained almost 58.53 ± 1.1% of the original volume while supporting bone formation compared with Test A (43.91 ± 1.2%; **Figs. 3d–f & Table 1**).

Histological description at eight weeks

Cortical defect closure: All groups showed an approximation of the borders and a subsequent reduction of the original critical-size defect. Test B showed the highest defect closure (68.71 ± 1.2%); a mixture of new bone and granules formed the new cortical bone. Test A showed partial closure (58.95 ± 3.4%) and the control group showed the lowest defect closure (11.23 ± 1.8%).

Figs. 3a–c

Figs. 3d–f

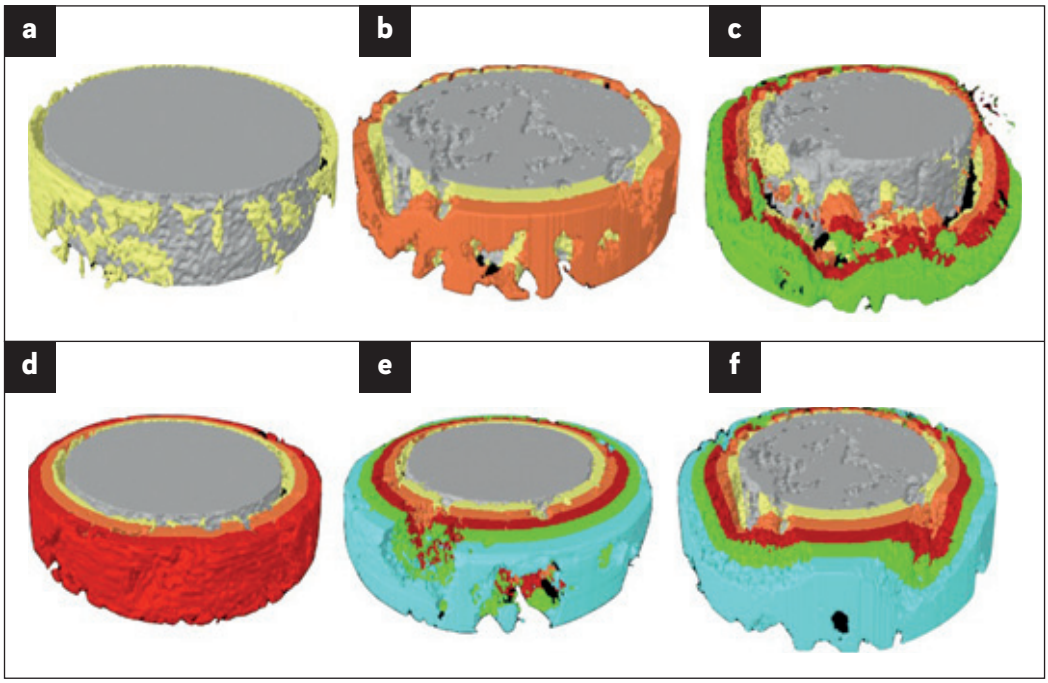

Figs. 3a–c
Micro-CT evaluation of the test groups at eight weeks.

The images represent a comparison between the two study times and the different materials tested. Dotted circles show the initial defect size, illustrating the reduction in graft volume in all groups. The control group is not shown, as control defects did not receive any graft material **(a)**. Test A showed an increased reduction in the graft volume **(b)**. Test B showed a medium-volume reduction **(c)**.

Figs. 3d–f
Micro-CT evaluation of the test groups at 12 weeks.

The images represent a comparison between the two study times and the different materials tested. Dotted circles show the initial defect size, illustrating the reduction in graft volume in all groups. The control group is not shown, as control defects did not receive any graft material **(d)**. Test A showed an increased reduction in the graft volume **(e)**. Test B showed a medium-volume reduction **(f)**.

Both test groups showed significant defect closure in comparison with the control group ($p < 0.05$; **Table 2**).

Residual material: Test B showed a higher percentage of residual material than did Test A ($p < 0.05$; **Table 2**).

Connective tissue: Connective tissue was higher in the control group (87.32 ± 1.4%) compared with Tests A and B ($p < 0.05$; **Figs. 4a–c & Table 2**).

New bone: New bone grew at the defect borders and between the particles in both Tests A and B. In the control group, new bone was only present at the defect borders. Bone formation commonly started in and around the 4BONE XBM graft particles. The highest amount of new bone was found in Test B, followed by Test A and the control group ($p < 0.05$; **Table 2**).

Histological description at 12 weeks

Under fluorescence microscopy, in both groups at 12 weeks of healing, the presence of a hard-tissue bridge that sealed the coronal part of the extraction socket was observed. The bridge was due to a continued small amount of new bone formation with some areas of mature bone. The material favored the growth of new bone in two different ways: first, by creating a new bridge between the defect walls and, second, through the actions of its components. At 12 weeks, the defect had completely closed in the group treated with 4BONE XBM plus 3% silicon compared with the group treated with 4BONE XBM alone. This marginal bridge was mainly of woven bone with areas of lamellar bone and some 4BONE XBM granules included inside the new bone **(Figs. 4d–f)**.

Table 2

Histomorphometry 8 weeks	**Cortical defect closure** (Mean ± S.D.)	**Residual material** (Mean ± S.D.)	**Connective tissue** (Mean ± S.D.)	**New bone** (Mean ± S.D.)
Control[a]	11.23 ± 1.8%	–	87.32 ± 1.4%*[b, c]	14.87 ± 1.5%
Test A[b]	58.95 ± 3.4%	44.33 ± 2.1%	16.67 ± 1.7%	41.33 ± 1.2%*[a]
Test B[c]	68.71 ± 1.2%*[b, a]	49.86 ± 3.2%*[b, a]	12.87 ± 1.1%	45.78 ± 1.9%*[a]

*Statistical significance was set at $p < 0.05$.

Table 2
Histomorphometry at eight weeks.

Post hoc multiple comparisons showed that cortical defect closure and residual material were higher for **Test B**, connective tissue was higher for the control group, and new bone formation was higher for **Tests A** and **B** in comparison with the control group.

Table 3
Histomorphometry in 12 weeks.

Post hoc multiple comparisons showed that defect closure and residual material were higher for **Test B**, connective tissue was higher for the control group, and new bone formation was higher for **Tests A** and **B** in comparison with the control group.

Table 3

Histomorphometry 12 weeks	Cortical defect closure (Mean ± S.D.)	Residual material (Mean ± S.D.)	Connective tissue (Mean ± S.D.)	New bone (Mean ± S.D.)
Control[a]	26.45 ± 1.5%	–	71.65 ± 1.6%*[b,c]	27.54 ± 2.1%
Test A[b]	78.23 ± 1.2%	34.36 ± 1.1%	14.28 ± 1.9%	53.29 ± 1.7%*[a]
Test B[c]	86.11 ± 1.9%*[b,a]	36.24 ± 1.8%*[b,a]	10.37 ± 1.6%	58.92 ± 0.8%*[a]

*Statistical significance was set at $p < 0.05$.

Cortical defect closure: All groups showed a reduction in the defect size in comparison with the eight-week study time. Test B showed the highest defect closure (86.11 ± 1.9%). Test A showed increased closure (78.23 ± 1.2%) in comparison with the eight-week study time, and the control group showed the lowest amount of defect closure (26.45 ± 1.5%). Both test groups showed significant defect closure in comparison with the control group ($p < 0.05$; **Table 3**).

Residual material: Test B showed a higher percentage of residual material (39.41 ± 1.3%) in comparison with Test A (35.78 ± 2.9%) and the control group ($p < 0.05$; **Table 3**).

Connective tissue: Connective tissue was the highest in the control group (71.65 ± 1.6%), and was lower in Tests A and B ($p < 0.05$; **Table 3 & Figs. 4d–f**).

New bone: New bone was observed at the centre of the defect and at the borders in Tests A and B; in the control group, no new bone formation was found. The highest amount of new bone was found in Test B, followed by Test A ($p < 0.05$; **Table 3**).

Discussion

The purpose of the present work was to evaluate the benefits of incorporating 3% silicon into the composition of a biphasic synthetic graft material of HA/β-TCP, used in critical-size defects in dogs' post-extraction defects. The current dog model has previously been used in several experiments in our laboratory to study various aspects of socket healing.[4–6] In the studies referred to, woven bone started to form in the fresh extraction socket after one week of healing and after four weeks the socket was largely filled with woven bone (about 90% of the socket).

In our present study, cortical defect closure was evaluated by histological and histomorphometric tests at eight and 12 weeks. Excellent defect closure in both test groups with graft material granules surrounded by new bone was found.

The present experiment demonstrated that the early healing of an extraction socket grafted with HA/β-TCP plus 3% silicon involved new bone formation and a coagulum was replaced by a provisional granulation tissue matrix in which new woven bone could be formed. The biphasic biomaterial was apparently involved in this process. HA granules were occupied by large active multinucleated cells that most likely removed calcium and phosphate ions from the small granules of the biomaterial. Thus, in the grafted sites, substantial amounts of newly formed bone could only be detected in the apical portion of the socket where the graft material was absent. In the remaining portions of the grafted sockets, a mildly inflamed provisional matrix surrounded the majority of the 4BONE XBM granules.

The present results agree with those obtained by El Backly et al., who compared the effects of platelet-rich plasma and a silicon-stabilized HA/β-TCP scaffold on healing critical-size defects in rabbit calvaria, evaluating healing at four, eight and 16 weeks.[24]

In the nongrafted control sites, large amounts of woven bone had formed in most compartments of the socket. This finding is in agreement with observations from similar experiments that investigated tissue modeling and remodeling in extraction sockets, as well as in mechanically produced defects in the alveolar ridge in dogs.[4, 5]

Most of the graft particles present in the test sites were surrounded by either a dense provisional matrix or newly formed woven bone, especially in the test group treated with 4BONE XBM plus 3% silicon. Most of the 4BONE XBM granules were in direct contact with immature woven bone.

The present study used CT and resin-embedded histology to evaluate healing evolution. The results showed that the silicon-stabilized

Figs. 4a–c

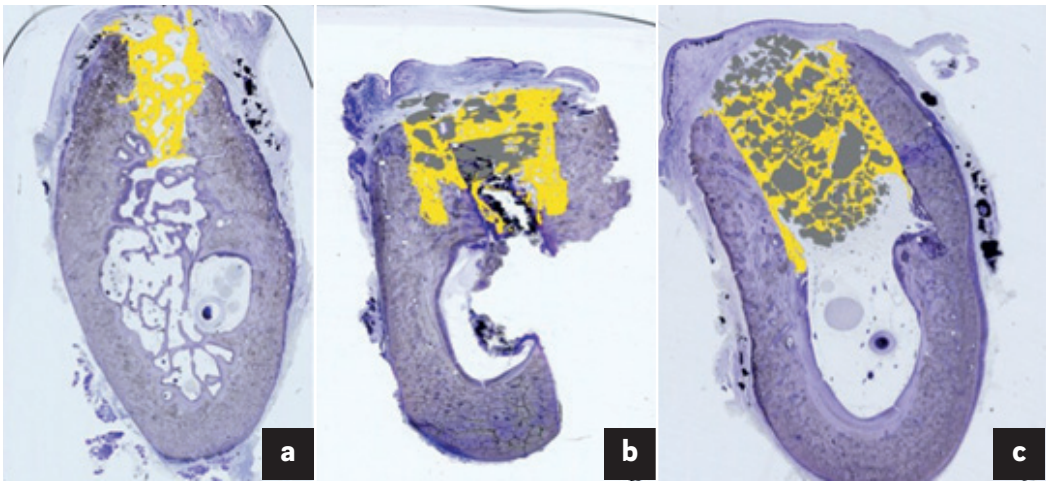

Figs. 4a–c Histomorphometric comparison at eight weeks between all groups.

Control defect: Bone formation was observed only at the defect walls, and incomplete closure of the defect was observed **(a)**.

Test A: Bone formation was observed around the periphery of the granules; at the basal zone, new cortical formation supported by the granules was observed **(b)**.

Test B: A reduction in the graft volume was observed, with increased bone formation around and inside the granules **(c)**.

Figs. 4d–f

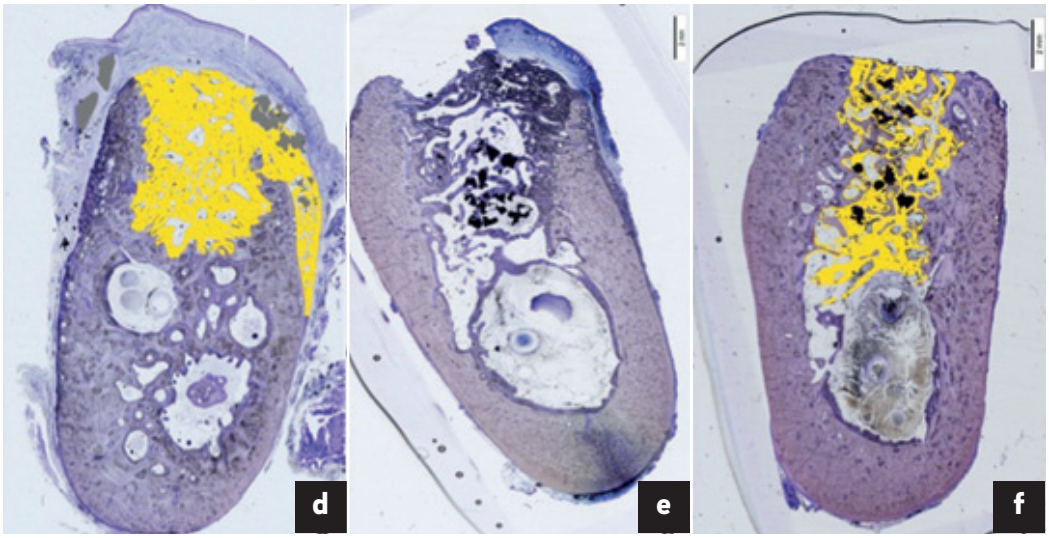

Figs. 4d–f Histomorphometric comparison at eight and 12 weeks between all groups.

Control defect: Bone formation was observed only at the defect walls, and complete closure of the defect was not observed **(d)**.

Test A: Bone formation was observed around the periphery of and inside the granules **(e)**.

Test B: A reduction in the graft volume was observed, with increased bone formation around and inside the granules **(f)**.

HA/β-TCP scaffold produced effective defect closure and improved new bone formation. The material was also very stable. These results agree with research carried out by Kruse et al., who created noncritical-size defects in rabbit calvarias, filling them with three different materials: synthetic HA/silica oxide-based test granules, xenogenic HA-based granules, and synthetic HA/silica oxide-based granules.[25] It was found that the incorporation of silica into the HA provided comparable results to a standard xenogenic bovine mineral in terms of bone formation and defect bridging in noncritical-size defects.

The residual material in the present study was higher in Test B, a finding that agrees with several other studies that have affirmed that incorporating calcium silicate into β-TCP cement increases the material's stability and mechanical properties. As demonstrated by Velasquez et al., the addition of silicon to the β-TCP ceramic structure enhanced its properties by reducing its resorption rate and thus increasing the material's stability during the bone formation processes.[12] Similar results were obtained by Wang et al.,[2] who suggest that 50 or 80% silicon could promote bone regeneration by stimulating osteogenesis, angiogenesis, and the proliferation and differentiation of osteoblast-like cells.[26]

The present study found connective tissue present in higher percentages in the control group in comparison with Tests A and B, which agrees with research carried out by De Aza et al., who implanted β-TCP and β-TCP doped with 3 wt% dicalcium silicate ceramic (β-TCPss) in critical-size defects in rabbit tibiae.[14] They observed organized collagen fibrils at the β-TCPss–bone interface for TCP doped with 3 wt% dicalcium silicate ceramic after four

weeks, whereas a collagen-free layer was present around the silicon-free β-TCP implants. These findings suggest that the incorporation of silicate ions into β-TCP ceramics promoted bone remodeling processes at the β-TCPss–bone interface, so that the stability rate of the β-TCPss material decreased.[14] Apparently, the organized collagen network facilitated the later mineralization of the collagen matrix, aided by the silica content. Moreover, the introduction of calcium silicate into porous TCP bioceramics is an effective way to prepare bioactive bone grafting scaffolds for clinical use and to control properties such as *in vivo* degradability and osteoinduction of TCP.[27]

In the present study, new bone formation was higher in Tests B and A in comparison with the control group, which showed maximum new bone formation after 12 weeks. These results agree with earlier studies incorporating different kinds of calcium silicate into synthetic ceramic cements. The incorporation of dicalcium silicate (C_2S) into the structure of β-TCP improved the materials' integration and compatibility, facilitating its capacity to bond with natural bone and improving the rate of new bone formation in comparison with a C_2S-free β-TCP composition.[12] According to Velasquez et al., the *in vivo* behavior of β-TCP ceramic and C_2S-doped β-TCP compositions matched their *in vitro* behavior.[12] The bioactivity and biocompatibility of these ceramics depended on their initial C_2S content. The results of the study suggest that doping of the β-TCP ceramic with 3% C_2S promotes bone mineralization during implantation into natural bone. Of all the compositions tested, the biphasic material doped with 3 wt% C_2S showed the greatest bioactivity both *in vitro* and *in vivo* and thus could be of interest for bone restorative purposes in specific applications.[12] It offers an ideal matrix in regenerative procedures and might be a promising candidate as an implant material in orthopedic, oral and maxillofacial applications owing to its mechanical and biological properties.[12]

Conclusion

Despite the limitations of this dog study, it may be concluded that the use of this biphasic material favors new bone formation and allows critical-size defects to heal without interfering in the regeneration process. The biphasic material with 3% silicon increased the dimensional stability of the graft, a feature that offers potential in areas that require dimensional stability and replacement by bone tissue.

Competing interests

The authors declare that they have no competing interests.

José Luis Calvo Guirado,[†]
Pérez Albacete Martínez Carlos,[†]
José Manuel Granero Marín,[†‡]
Rafael Arcesio Delgado Ruiz,[†§]
Maria Piedad Ramírez Fernández,[†‡]
José Eduardo Maté Sánchez de Val[†]
Gerardo Gómez Moreno[†**]

[†] International Dentistry Research Cathedra, Universidad Católica San Antonio de Murcia, Murcia, Spain

[‡] Faculty of Medicine and Dentistry, University of Murcia, Spain

[§] Department of Prosthodontics and Digital Technology, Stony Brook University, School of Dental Medicine, Stony Brook, N.Y., U.S.

[**] Department of Pharmacological Interactions, Faculty of Dentistry, University of Granada, Spain

Corresponding author:

Prof. José Luis Calvo Guirado
Calle Mozart, 4, 1º C–D
30002 Murcia
Spain

T +34 968 26 8353
F +34 968 26 8353
jlcalvo@ucam.edu

References

1.
Schropp L, Wenzel A, Kostopoulos L, Karring T. Bone healing and soft tissue contour changes following single-tooth extraction: a clinical and radiographic 12-month prospective study.
→ Int J Periodontics Restorative Dent.
2003 Jul-Aug;23(4):313–23.

2.
Wang C, Lin K, Chang J, Sun J. The stimulation of osteogenic differentiation of mesenchymal stem cells and vascular endothelial growth factor secretion of endothelial cells by β-$CaSiO_3$/β-$Ca_3(PO_4)_2$ scaffolds.
→ J Biomed Mater Res A.
2014 Jul;102(7):2096–104.

3.
Becker W. Treatment of small defects adjacent to oral implants with various biomaterials.
→ Periodontol 2000.
2003 Oct;33(1):26–35.

4.
Cardaropoli G, Araújo MG, Lindhe J. Dynamics of bone tissue formation in tooth extraction sites: an experimental study in dogs.
→ J Clin Periodontol.
2003 Sep;30(9):809–18.

5.
Araújo MG, Lindhe J. Dimensional ridge alterations following tooth extraction: an experimental study in the dog.
→ J Clin Periodontol.
2005 Feb;32(2):212–8.

6.
Araújo M, Linder E, Lindhe J. Effect of a xenograft on early bone formation in extraction sockets: an experimental study in dog.
→ Clin Oral Implants Res.
2009 Jan;20(1):1–6.

7.
Araújo MG, Liljenberg B, Lindhe J. β-tricalcium phosphate in the early phase of socket healing: an experimental study in the dog.
→ Clin Oral Implants Res.
2010 Apr;21(4):445–54.

8.
Araújo MG, Liljenberg B, Lindhe J. Dynamics of Bio-Oss Collagen incorporation in fresh extraction wounds: an experimental study in the dog.
→ Clin Oral Implants Res.
2010 Jan;21(1):55–64.

9.
Nomura T, Katz JL, Powers MP, Saito C. Evaluation of the micromechanical elastic properties of potential bone-grafting materials.
→ J Biomed Mater Res B Appl Biomater.
2005 Apr;73B(1):29–34.

10.
Schwarz F, Herten M, Ferrari D, Wieland M, Schmitz L, Engelhardt E, Becker, J. Guided bone regeneration at dehiscence-type defects using biphasic hydroxyapatite + beta tricalcium phosphate (Bone Ceramic) or a collagen-coated natural bone mineral (BioOss Collagen): an inmunohistochemical study in dogs.
→ Int J Oral Maxillofac Surg.
2007 Dec;36(12):1198–206.

11.
Pérez Sánchez MJ, Ramírez Glindon E, Lledó Gil M, Calvo Guirado JL, Pérez Sánchez C. Biomaterials for bone regeneration.
→ Med Oral Patol Oral Cir Bucal. 2010 May;15(3):e517–22.

12.
Velasquez P, Luklinska ZB, Meseguer Olmo L, Maté Sánchez de Val JE, Delgado Ruiz RA, Calvo Guirado JL, Ramírez Fernández MP, De Aza PN. αTCP ceramic doped with dicalcium silicate for bone regeneration applications prepared by powder metallurgy method: *in vitro* and *in vivo* studies.
→ J Biomed Mater Res A.
2013 Jul;101A(7):1943–54.

13.
Dutta-Roy T, Simon JL, Ricci JL, Rekow ED, Thompson VP, Parsons JR. Performance of hydroxyapatite bone repair scaffolds created via three-dimensional fabrication techniques.
→ J Biomed Mater Res A.
2003 Dec;67A(4):1228–37.

14.
De Aza PN, Luklinska ZB, Maté Sánchez de Val JE, Calvo Guirado JL. Biodegradation process of α-tricalcium phosphate and α-tricalcium phosphate solid solution bioceramics *in vivo*: a comparative study.
→ Microsc Microanal.
2013 Oct;19(5):1350–7.

15.
Cardaropoli D, Cardaropoli G. Preservation of the postextraction alveolar ridge: a clinical and histologic study.
→ Int J Periodontics Restorative Dent.
2008 Sep-Oct;28(5):469–77.

16.
Calvo Guirado JL, Gómez Moreno G, Barone A, Cutando A, Alcaraz Baños M, Chiva F, López Marí L, Guardia J. Melatonin plus porcine bone on discrete calcium deposit implant surface stimulates osteointegration in dental implants.
→ J Pineal Res.
2009 Sep;47(2):164–72.

17.
Calvo Guirado JL, Gómez Moreno G, López Marí L, Guardia J, Marínez González JM, Barone A, Tresguerres IF, Paredes SD, Fuentes Breto L. Actions of melatonin mixed with collagenized porcine bone versus porcine bone only on osteointegration of dental implants.
→ J Pineal Res.
2010 Apr;48(3):194–203.

18.
Tadic D, Epple M. A thorough physicochemical characterisation of 14 calcium phosphate-based bone substitution materials in comparison to natural bone.
→ Biomaterials.
2004 Mar;25(6):987–94.

19.
Maté Sánchez de Val JE, Calvo Guirado JL, Delgado Ruiz RA, Ramírez Fernández MP, Negri B, Abboud M, Martínez IM, De Aza PN. Physical properties, mechanical behavior, and electron microscopy study of a new α-TCP block graft with silicon in an animal model.
→ J Biomed Mater Res A.
2012 Dec;100A(12):3446–54.

20.
Zou S, Ireland D, Brooks RA, Rushton N, Best S. The effects of silicate ions on human osteoblast adhesion, proliferation, and differentiation.
→ J Biomed Mater Res B Appl Biomater.
2009 Jul;90B(1):123–30.

21.
Beck GR Jr, Ha SW, Camalier CE, Yamaguchi M, Li Y, Lee JK, Weitzmann MN. Bioactive silica-based nanoparticles stimulate bone-forming osteoblasts, suppress bone-resorbing osteoclasts, and enhance bone mineral density *in vivo*.
→ Nanomedicine.
2012 Aug;8(6):793–803.

22.
Martínez IM, Velásquez P, De Aza PN. Synthesis and stability of α-tricalcium phosphate doped with dicalcium silicate in the system $Ca_3(PO_4)_2$–Ca_2SiO_4.
→ Mater Charact.
2010 Jul;61(7):761–7.

23.
Urbaniak GC, Plous S. Research Randomizer [Internet-based computer software].
→ Version 4.0.
[cited 2015 May 8]. 2013.
Available from:
http://www.randomizer.org/.

24.
El Backly RM, Zaky SH, Canciani B, Saad MM, Eweida AM, Brun F, Tromba G, Komlev VS, Mastrogiacomo M, Marei MK, Cancedda R. Platelet rich plasma enhances osteoconductive properties of a hydroxyapatite-β-tricalcium phosphate scaffold (Skelite) for late healing of critical size rabbit calvarial defects.
→ J Craniomaxillofac Surg.
2014 Jul;42(5):e70–9.

25.
Kruse A, Jung RE, Nicholls F, Zwahlen RA, Hämmerle CHF, Weber FE. Bone regeneration in the presence of a synthetic hydroxyapatite/silica oxide-based and a xenogenic hydroxyapatite-based bone substitute material.
→ Clin Oral Implants Res.
2011 May;22(5):506–11.

26.
Fei L, Wang C, Xue Y, Lin K, Chang J, Sun J. Osteogenic differentiation of osteoblasts induced by calcium silicate and calcium silicate/β-tricalcium phosphate composite bioceramics.
→ J Biomed Mater Res B Appl Biomater.
2012 Jul;100B(5):1237–44.

27.
Liu S, Jin F, Lin K, Lu J, Sun J, Chang J, Dai K, Fan C. The effect of calcium silicate on *in vitro* physiochemical properties and *in vivo* osteogenesis, degradability and bioactivity of porous β-tricalcium phosphate bioceramics.
→ Biomed Mater [Internet].
2013 Apr [cited 2015 May 4];8(2):025008. doi: 10.1088/1748-6041/8/2/025008.